# A new multiple-PRT scheme for Météo-France Doppler radar network to improve spectral moment estimation of weather radar signal and ground clutter filtering.

Mohammed TAHANOUT, *LTIR, USTHB University, Algiers, Algeria.* Jacques PARENT DU CHATELET and Clotilde AUGROS *Météo-France, Trappes, France.*
mtahanout@gmail.com . jacques.parent-du-chatelet@meteo.fr

## Abstract

This work describes a new staggered pulse repetition time (PRT) scheme design to enhance spectral processing of weather radar signal, to improve Doppler velocities dealiasing, and to filter-out ground clutter in Météo-France Doppler radar network "ARAMIS". This network is currently working with a triple-PRTs scheme and ± 60 $m.s^{-1}$ extended Nyquist interval. The problem of power spectrum recovering, and ground clutter filtering, with dual PRT scheme has been studied by Sachidananda and Zrnic in 2000. They have developed an algorithm based on magnitude deconvolution procedure using a matrix inversion. This algorithm was tested successfully on the research and development radar WSR-88D. Trying to apply this algorithm to our C-band triple PRT scheme ($T_1$ = 2.64 ms, $T_2$=3.08 ms and $T_3$= 3.3 ms), we experienced problems as far as the spectral width $\sigma_v$ is bigger than approximately 1 $m.s^{-1}$.
To overcome these difficulties and make a good estimation of the weather radar spectrum, particularly in the ARAMIS context, we have developed a new method based on an optimization of the radar transmission scheme to reach a large number of points of the autocorrelation function $R(\tau)$. Basically, a dual PRT scheme gives 3 points of $R(\tau)$ for time lags $0,T_1$ and $T_2$ ; a triple PRT scheme gives 4 points of $R(\tau)$ for time lags $0,T_1$, $T_2$ and $T_3$. A multiple-PRT scheme can reach (n+1) points of $R(\tau)$ for time lags $0,T_1$, $T_2$ … $T_n$. Additional points can also be obtained for combined lags ($T_1+T_2$, $T_2+T_3$,…). Choosing $T_{i+1} = (T_i + T_u)$, the function $R(\tau)$ is available over the interval $[T_1 , \Sigma Ti - T_1]$ with a uniform sampling time $T_u$. $R(\tau)$ is forced to zero for the other time lags and the power spectrum simply recovered using classical FFT algorithm within an extended Nyquist interval of $\lambda (2 T_u)^{-1}$. This power spectrum is convolved by the sinc function which is the power spectrum of the time window ($\Sigma T_i - 2 T_1$).

## 1. Introduction

In operational weather radar remote sensing, we generally attempt to measure reflectivity at large distances, up to 250 km for C-band or S-band. This leads to quite large PRTs (Pulse Repetition Time, or the time between radar pulses) which correspond to quite weak unambiguous Doppler velocities. This well known "Doppler-Range dilemma" can be expressed by :

$$v_a = \pm \frac{\lambda}{4T} \quad (1)$$

where $v_a$ is the Nyquist Doppler velocity, T the PRT and $\lambda$ the radar wavelength. Taking for example the operational Météo-France C-band radars, for which T = 3 ms, the Nyquist velocity is equal to ± 5 m/s, which is much smaller than the expected maximum horizontal rain velocity. According to equation (1), the Nyquist velocity can be increased by decreasing T, but to the expense of the maximum range, or unambiguous range $r_a$ which is given by $r_a = cT/2$. Combining with (1), we obtain $v_a r_a = c \lambda/8$ which governs the relation between $v_a$ and $r_a$.
To mitigate these ambiguity problems, Zrnic and Mahapatra proposed in 1985 a new "dual PRT" technique, or staggered PRT, which consists to transmit radar pulses separated alternatively by two PRTs T1 and T2. The extended Nyquist velocity is then given by $\lambda/[4(T_2 - T_1)]$ and the smallest range by $c[\min(T_1, T2)]/2$. This technique is much more adapted for the pulsed-radars, particularly for magnetron-based radars. More recently, Meteo-France proposed (Tabary et al. 2005 and Tabary et al, 2006) a triple-PRT scheme which has been operationally implemented in the French ARAMIS radar network. This last scheme is optimized to work with C- and S-band radars over a large extended-Nyquist interval of ± 60 m/s.

Unfortunately, these Multiple-PRT techniques lead to backscattered signals time-series, which are not uniformly sampled in time. And it is difficult to perform spectral analysis or ground clutter filtering with such time series. In fact, these signals are convolved in the spectral domain by a lot of spectral lines repeated all over the extended Nyquist interval with various magnitudes. The ground clutter and rain signatures can be severely mixed together. Despite these difficulties, Sachidananda and Zrnic proposed in 2000 a magnitude deconvolution algorithm adapted to restore power spectra for the S-band WSR-88D radars: using the dual PRT technique implemented in these radars, the ground clutter spectrum only presents 4 replicas over the Nyquist interval of ± 50 m/s (Sachidananda et al. 2000). The spectral moments are estimated after deconvolution, and the ground clutter spectral components (basically 4 spectral lines) are simply removed from the spectrum before deconvolution, removing also a part of the desired weather spectrum. Because of the overlaps, this technique works well only for spectrum width lower than 6 m/s.
In the triple-PRT scheme used by Meteo-France, the ground clutter has much more replicas. For example, using a C-band radar with a mean PRT of 3 ms, the number of replicas is as high as 40. In this case, the Sachidananda and Zrnic algorithm gives very bad results for spectral width beyond 1 m/s.

## 2. Description of the Multiple-PRT Method

The new approach that we describe in this paper aims to overcome this limitation, to avoid the replicas in the extended Nyquist domain, and to estimate the Doppler weather spectrum.
It is based on the optimization of the radar transmission scheme to reach a large number of points of the autocorrelation function $R(\tau)$, in order to improve spectral analysis of the observed phenomenon. Mainly, the dual and triple PRT techniques mentioned above compute

respectively two and three coefficients of the autocorrelation function, at lags ($T_1$, $T_2$) for the dual PRT (Torres et al. 2002) and ($T_1$, $T_2$, $T_3$) for the triple PRT (Tabary et al, 2006), and these coefficients are used to estimate the observed phenomenon radial velocity by a pulse pair method. Even if they are not used in the pulse pair method, additional $R(\tau)$ coefficients could also be available for combination like ($T_1$+$T_2$), ($T_1$+$T_3$), ($T_2$+$T_3$), ($T_1$+$T_2$+$T_3$), etc… to obtain a better filling of $R(\tau)$ (see figure 1). But some hole remains, for example between $T_3$ and ($T_1$+$T_2$), and the spectrum computed with this type of autocorrelation function is infected with strong replicas due to the lack information in the received signal resulting in zeros values in the autocorrelation function $R(\tau)$.

The new idea is to implement a multiple PRT scheme ($T_1$, $T_2$,… $T_n$,) specifically designed to give as many as possible coefficients of the autocorrelation function, for time lags $T_1$, $T_2$,… $T_n$ etc.. Some basic remarks must be given:

- $T_1$ being the smaller PRT, $R(\tau)$ cannot be computed for time lags in the time interval [$-T_1$ , $+T_1$] (except for time lag 0).
- The multiple PRT scheme is periodic, with a period equal to $\Sigma T_i$. Consequently, the $R(\tau)$ sampling function is also periodic with the same period, and $R(\tau)$ cannot be computed for time lags in the interval [$\Sigma T_i - T_1$ , $\Sigma T_i + T_1$] (except for time lag equal to $\Sigma T_i$).
- if the time interval $T_u$ between successive PRTs is constant, ($T_u$=$T_{i+1}$–$T_i$), the available autocorrelation coefficients are uniformly distributed between $T_1$ and $T_n$.
- the autocorrelation function will be uniformly sampled only if the PRTs are integers multiples of $T_u$ :

$$T_i = n_i\, T_u \qquad (2)$$

- the value of $T_u$ determines the extended Nyquist interval by $v_a = \lambda/(4T_u)$.
- the smaller PRT $T_1$ determines the unambiguous range $r_a = cT_1/2$.

*ideal PRT scheme*

For a given extended Nyquist interval $V_a$, and a given maximum range $r_a$, the *"ideal PRT scheme"* will permit to compute all the autocorrelation coefficients between $T_1$ and ($\Sigma T_i - T_1$), regularly separated by the time-step $T_u$.

For such an *"ideal PRT scheme"*, the power spectrum is easily recovered by applying a classical FFT algorithm on the autocorrelation function windowed by a $\Delta T = (\Sigma T_i - 2T_1)$ rectangular function. The obtained spectrum is the result of the true Doppler spectrum convolved by the power spectrum of the window. The spectral lines are broadened by $1/\Delta T$ and the Doppler spectrum suffers from secondary sinx/x lobes which can be reduced by applying some well-known weighting functions (Hamming, Hanning, …).

It is important to note that, for spectral width $\sigma_v$ much larger than $\lambda/(2T_1)$, the correlation time $T_c$ is much shorter than $T_1$, and the autocorrelation function has significant values only for time lags $-T_c < \tau <+ T_c$ which are not accessible with the considered multiple PRT scheme: the power spectrum cannot be computed, neither the Doppler-wind. But this limitation is not from the method: it is just a sampling problem: spectral width $\sigma_v$ are accessible only with sampling times lower than $\lambda/(2\sigma_v)$.

The quality of the estimation of the autocorrelation coefficients depends on the number of independent individual values averaged to get the coefficients. Given the dwell time $T_d$, which is the amount of time used for spectral analysis for each pixel, the total number $M_T$ of individual measurement contributing to the correlation coefficients is approximately: $M_T = N_P\,(T_d / \Sigma T_i)$, where $\Sigma T_i$ is the multiple PRT scheme period, and $N_P$ the number of range gates used in the average.

For example, with a $5°sec^{-1}$ rotating speed, a 3ms averaged PRT, a 7 PRTs scheme, and a 150m range resolution, it is straightforward to compute that, for each 1°-1km pixel, more than 60 individual measurements contribute to each coefficient of the autocorrelation function in C-band radar.

*real PRT scheme*

The "*ideal PRT scheme"* is not always accessible, and $R(\tau)$ will not be available for some points of the time interval [$T_1$, $\Sigma T_i - T_1$]. Then the spectrum will be convolved, not only by the rectangular function of $\Delta T$ width, but by this function with additional zero values due to the holes in $R(\tau)$. This will result in additional spectral lines and/or spectral broadening.

To get a scheme as close as possible to the "*ideal PRT scheme"*, it can be useful to rearrange the PRT sequence: the monotonic order is not required for the $T_i$ sequence. It can also be useful to repeat some values in the sequence.

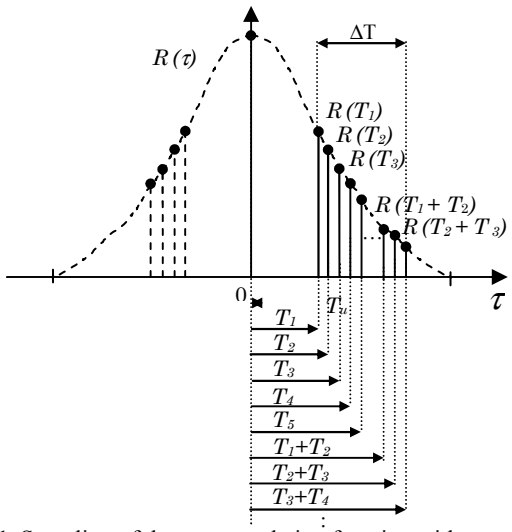


**Fig.1.** Sampling of the autocorrelation function with a multiple-PRT Scheme.

*Normalization of the autocorrelation function $R(\tau)$*

The autocorrelation coefficients are basically computed as follow:

$$R(\tau_l) = \frac{1}{M_l} \sum_{k=0}^{M_l - 1} s^*(k)\, s(k+l) \qquad (3)$$

$l$ represent the time lag shift number such as: $\tau_0 = 0$, $\tau_1 = T_1$, $\tau_2 = T_2$, …, $\tau_n = T_n$, $\tau_{n+1} = T_1 + T_2$, $\tau_{n+2} = T_1 + T_3$, …,

$\tau_{2n-1} = T_1 + T_n, \ldots$ Because of the non-uniform sampling, the number of samples $M_l$ used to compute each coefficient at a given time lag $l$ is variable. The maximum is at zero-lag where all samples contribute to the average.
To simplify the autocorrelation function computation with FFT algorithms, we can use the zeros-padding formalism proposed by (Sachidananda et al. 2000): we consider the sampled signal $s_{sam}(k)$ as the product of the real signal $s(k)$ by a binary logic code sequence representing the sampling function of the radar pulses $\psi(k)$ (fig.2) which is equal to 1 on the available samples (red points on the figure), to zero elsewhere (black points on the figure) :

$$s_{sam}(k) = s(k)\ \psi(k) \qquad (4)$$

$s_{sam}(k)$ and $\psi(k)$ are both uniformly sampled at $T_u$, and it is straightforward to compute their autocorrelation function $R_{sam}$ and $R_\psi$ with classical FFT algorithms. For the no-zero values, they are related by :

$$R_n(\tau) = \frac{R_{sam}(\tau)}{R_\psi(\tau)} \qquad (5)$$

where $R_{sam}(\tau)$ is the autocorrelation function of the signal up-sampled with zero padding.

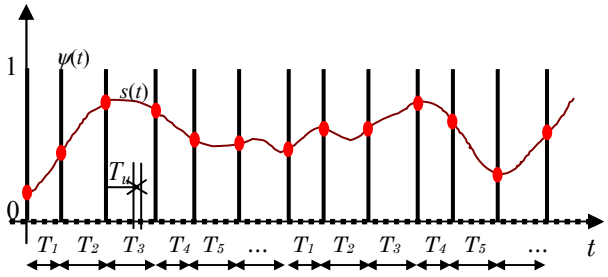


**Fig.2.** Weather signal Sampled with multiple PRT pulses.

The non zero values of $R_\psi$ are equal to the numbers $M_l$ of eq. (3) and, to compute the signal power spectrum, the following operations can be performed:
- $R_\psi(\tau)$ computation with FFT algorithm
- $R_{sam}(\tau)$ computation with FFT algorithm
- $R_n(\tau)$ computation by applying the eq. (5) normalization
- power spectrum by applying FFT on $R_n(\tau)$

### 3. Simulation results

We present in this section some simulations done to demonstrate the performances of the method to estimate the weather Doppler spectrum.

The signal is simulated within spectral domain in a desired extended Nyquist interval of 2 $v_N$ considering a Gaussian spectrum shape centered on a mean velocity $v_m$ and cover a spectral width of $\sigma_v$. The spectrum is computed with velocity step resolution of $v_u$. Power spectral components of a white noise are added in the whole extended Nyquist interval. The level of these components is tuned according to the needed SNR. The $I$ and $Q$ discrete time series of the simulated received in phase-quadrature time signal $s(k) = I(k) + j\ Q(k)$ are produced by applying the inverse Fast Fourier Transform (Zrnic, 1975). These time series are then re-sampled with non-uniform sampling period according to the chosen PRT scheme.
In these simulations we choose to compare the performances of spectral recovery of : (i) a multiple-PRT scheme, and (ii) the optimum Meteo-France triple-PRT scheme (Tabary et al. 2006). The weather spectrum is simulated in ± 26 m s$^{-1}$ Nyquist interval in both triple-PRT and 7-PRT schemes, which corresponds to a $T_u$ increment of 0.5ms. The two schemes time periods are detailed in Table 1.

TABLE 1. Multiple-PRT scheme parameters. The periods $T_i$ are given in ms.

| Triple-PRT | | 7-PRT scheme | |
|---|---|---|---|
| $T_1 = 2.5$ | $n_1 = 5$ | $T_2 = 3.0$ | $n_1 = 6$ |
| $T_2 = 3.0$ | $n_2 = 6$ | $T_1 = 2.5$ | $n_2 = 5$ |
| $T_3 = 3.5$ | $n_3 = 7$ | $T_3 = 3.5$ | $n_3 = 7$ |
| $T_u = 0.5$ms | | $T_2 = 3.0$ | $n_4 = 6$ |
| $T_i = n_i T_u$ | | $T_4 = 4.0$ | $n_5 = 8$ |
| ($n_i$ integer) | | $T_5 = 4.5$ | $n_6 = 9$ |
| | | $T_6 = 5.0$ | $n_7 = 10$ |

Even if a better scheme could be founded, we decided to test here a 7-PRT scheme with suffers from 6 isolated zero-coefficients (holes) in the autocorrelation function in the interval $[T_1, T_1+\Delta T]$. We note that, if the number of holes is small, and if they are isolated, the missing $R(\tau)$ coefficients can easily be interpolated.
The same unambiguous range of 375km is imposed for both schemes, leading to a minimum PRT $T_1$=2.5ms. The dwell time is fixed to 200ms, which corresponds to 1° in azimuth with the 5°sec$^{-1}$ antenna rotating speed. The corresponding spectral accuracy is 0.1m s$^{-1}$.

*Simulated Doppler spectrum and autocorrelation R(τ)*
Figure 3a shows a simulated Doppler spectrum example for a weather signal mixed with ground clutter. This spectrum presents a ground clutter spectral component (radial-velocity = 0, $\sigma_v$ = 0.2 m s$^{-1}$ ) and a weather signal (Gaussian shape Doppler spectrum, radial-velocity = + 12 m s$^{-1}$, $\sigma_v$ = 0.7 m s$^{-1}$). A noise signal is added with a SNR = 20 dB.

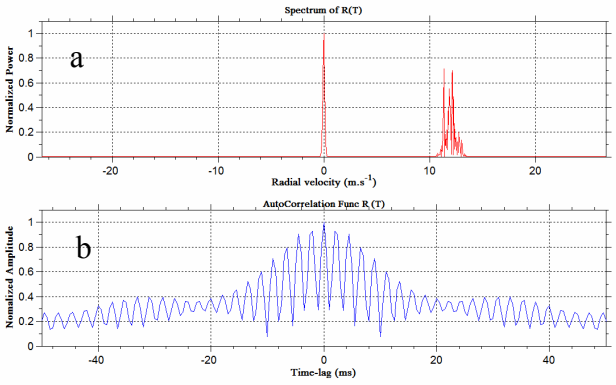


**Fig.3.** Simulation of a weather signal mixed with ground clutter echoes. (a) Simulated Doppler Spectrum in ± 26 m s$^{-1}$ extended Nyquist interval. (b) Corresponding autocorrelation function.

The corresponding true autocorrelation function $R_u(\tau)$ is given on fig.3b. The function $R_u(\tau)$ have been computed between ± 100 ms time lags corresponding to the dwell time, but it is shown only between -50 to 50ms to reveal its main components.

*autocorrelation and spectrum for a triple PRT scheme*

The normalized autocorrelation function $R_n(T)$, obtained after sampling the same signal with the triple-PRT scheme, is given on fig.4a. There are some similarities between the envelope of $R_n(T)$ and $R_u(T)$, but $R_n(T)$ is characterized by discontinuities (holes of zero-coefficients) due to the triple-PRT non-uniform sampling. In fact this function is known only for the time-lags: 0, $T_1$, $T_2$, $T_3$, and for combination of different additions between the previous lags such $T_1+T_2$, $T_1+T_3$, $T_2+T_3$, $T_1+T_2+T_3$, etc, in the whole time lags domain.

In the spectral domain, these discontinuities lead to spectral repetition, introducing a lot of velocity ambiguities : as shown in the fig.4b the ground clutter and the weather spectra obtained from $R_{sam}(T)$ are repeated over the whole extended Nyquist interval between ± 26 m s$^{-1}$ for each interval of $\lambda/(2\,(T_1+T_2+T_3))$. In this example, this interval is about 3 m s$^{-1}$. Consequently, the weather spectrum is mixed with the spectral replicas of the ground clutter, and it could be difficult to separate the different contributions.

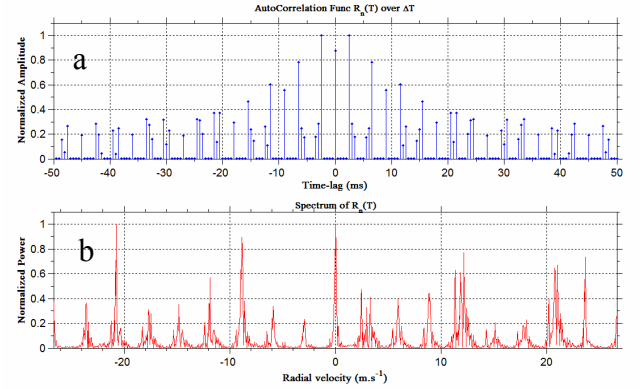


**Fig.4.** Same signal than fig. 3, but sampled with a triple-PRT scheme. (a) The autocorrelation function. (b) The triple-PRT spectrum in ± 26 m s$^{-1}$ extended Nyquist interval.

*Doppler spectrum if $R(\tau)$ is limited to $[T_1\text{-}T_3]$ interval*

If we limit the autocorrelation to the 3 first coefficients at lags $T_1$, $T_2$ and $T_3$ (dashed box in figure 5a), the corresponding spectrum is quite large (figure 5b) but the spectral position of the weather spectrum can still be located. The obtained spectrum is the true weather spectrum convolved with a sinc function. And the spectral width of this function is inversely proportional to $\Delta T = T_3 - T_1$ ($\Delta T \approx 0.66$ ms). The localization of the local maximum gives approximately the mean velocity of the Gaussian shape spectrum (Cho and al. 2005), but it is biased by the ground spectral line. For this particular example fig.4b, the bias on the mean velocity of the weather Doppler spectrum is about + 6 m.s$^{-1}$, but other simulations not presented here show that in some cases, this bias can increase up to ±10 m.s$^{-1}$.

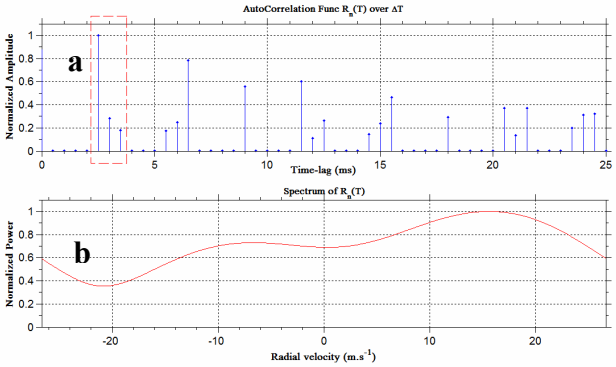


**Fig.5.** Same signal than fig. 3 or fig. 4, sampled with a triple-PRT scheme. (a) The three first coefficients of the autocorrelation function (in red dashed area). (b) Doppler spectrum computed using only these 3 first coefficients, in ± 26 m s$^{-1}$ Nyquist interval.

*Autocorrelation and spectrum for a 7 PRT scheme*

The spectral accuracy can be improved by increasing the $\Delta T$ time interval on which the autocorrelation function is uniformly sampled. This can be achieved very simply by increasing the number of PRTs interlaced in the scheme.

The autocorrelation function $R_n(T)$ given in fig.6a is computed with a 7-PRT scheme with $T_i = T_{i-1} + T_u$ ($i$= 2, 3, … ,7). As in the triple-PRT case, this function presents some discontinuities, but with much less zero-coefficients (holes). The power spectrum associated to $R_n(T)$ is shown in fig.6b. The ground clutter and weather components are clearly visible on the spectrum and the improvement is very clear with respect to the triple PRT case (fig 4b). But significant replica still exist (around +20m/s for example).

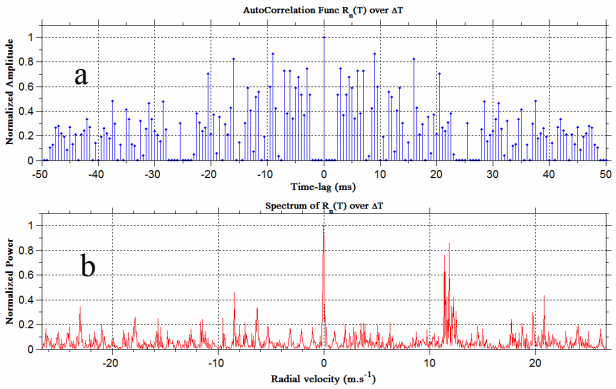


**Fig.6.** Doppler spectrum estimated using the autocorrelation function obtained with 7-PRT scheme sampling of the simulated signal corresponding to the spectrum given in fig.3. (a) The autocorrelation function. (b) The 7-PRT spectrum in ± 26 m s$^{-1}$ extended Nyquist interval.

*Doppler spectrum for a 7 PRT scheme if $R(\tau)$ is limited to $[T_1, \Delta T - 2T_1]$*

To avoid the replicas, the spectrum is computed using only the interval where the autocorrelation function $R_n(T)$ is uniformly sampled from lag $T_1$ (fig.7a). In this case, $\Delta T \approx$ 23.5 ms. The resulting spectrum is the effect of convolution of the true spectrum with sinc function less

wide than in Triple-PRT example. Thus, as shown in the fig.7b, the localization of the both weather spectrum and ground clutter can be done quite efficiently. In this example, the bias of localization of the weather mean radial velocity is about + 0.6 m $s^{-1}$ and 0 for the ground clutter. Moreover, the possibility of separation between the two spectra is improved.

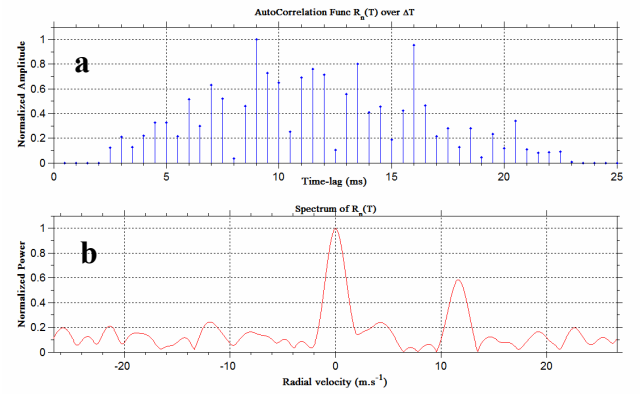


**Fig.7.** Doppler spectrum estimated using 41 coefficients of the autocorrelation function (uniform sampled part) obtained with 7-PRT scheme sampling of the simulated radar returns signal. (a) the Coefficients of the autocorrelation function available between 0ms and 25ms. (b) Corresponding spectrum in the ± 26 m $s^{-1}$ Nyquist interval.

## 4. Experimental Results

To test and validate our method, we have made up a 7-PRT scheme experiment with the Abbeville operational C-band radar. The test has been performed with the same parameters than defined in the simulation procedure (table 1). I and Q time series were recorded in June and July 2009 in both triple- and 7-PRT scheme.

The experiment was performed in a specific azimuthal-range sector characterized by significant ground clutter close to the radar. This area is located 10 km from the radar between 45° to 80° in azimuth and spread over 20 km in distance (fig. 8). The rotation velocity is set to 5°/s with elevation angle of 0.4°.

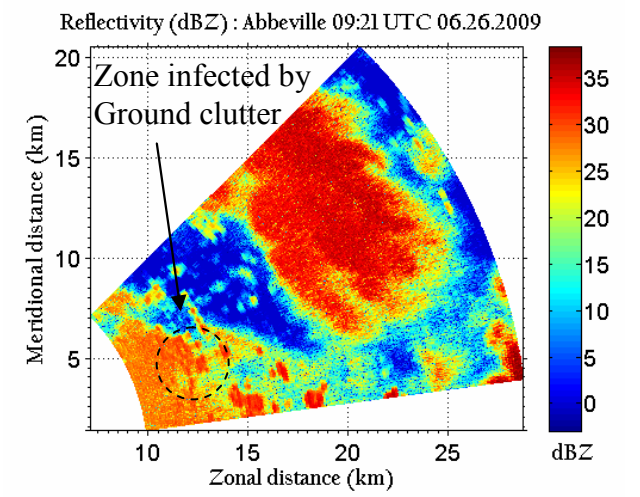


**Fig. 8.** Polar coordinate representation of the reflectivity (dBZ) due to rain and ground clutter in the experimental area. Range gates every 150m, elevation angle = 0.4°.

Figure 9 represents the estimated radial velocity of the sequence given in the fig.8. This result is obtained by applying the operational dealiasing algorithm developed for the 7-PRT scheme. Each pixel represents the estimated velocity within 1 km x 1° polar coordinates. As shown in the figure, the classic dealiasing algorithm does not detect the rain Doppler information though the presence of rain and gives 0 velocity which is the characteristic of the ground clutter in this area (within dashed circle).

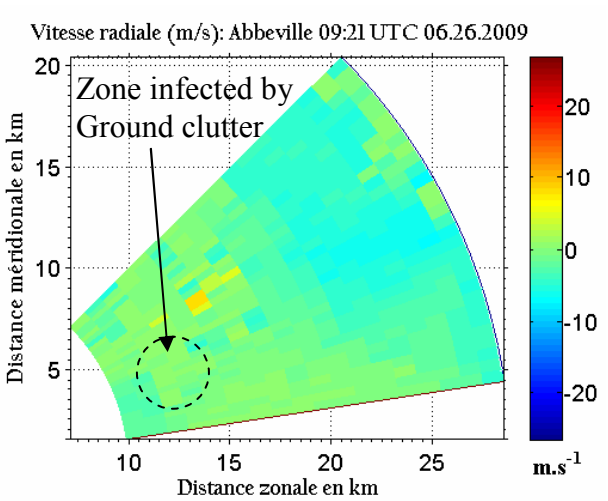


**Fig. 9.** Polar coordinate representation of the radial velocity (1 km x 1°) in the experimental area.

To reveal the presence of rain with non-zero velocity, we have plotted on figure 10 a 7-PRT Doppler spectrum in the ground clutter area (range=13 km and azimuth= 67°). In this example, the ground clutter narrow spectral line at 0 Doppler velocity is very clear. Some other narrow lines probably come from ground clutter replicas, a more wide spectral structure, close to –2m/s, may be due to rain.

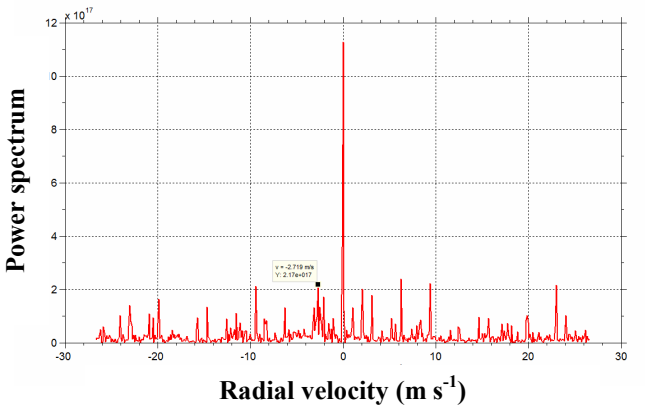


**Fig.10.** Example of a Doppler spectrum of weather radar signal returns mixed with a ground clutter echoes obtained with 7-PRT scheme pulses emission sequences.

The spectrum of figure 11 has been obtained, with the 7-PRT scheme, and using only the uniform part of the autocorrelation function. We observe that, as expected from simulation, the spectral representation is significantly improved: the two contributions, from ground clutter (at zero Doppler), and from rain (at minus 2.7m $s^{-1}$), are clearly visible. Some residual spectral lines,

probably due to the sinc secondary lobes, can also be reduced by applying a Hamming function on the autocorrelation function before FFT (figure 12).

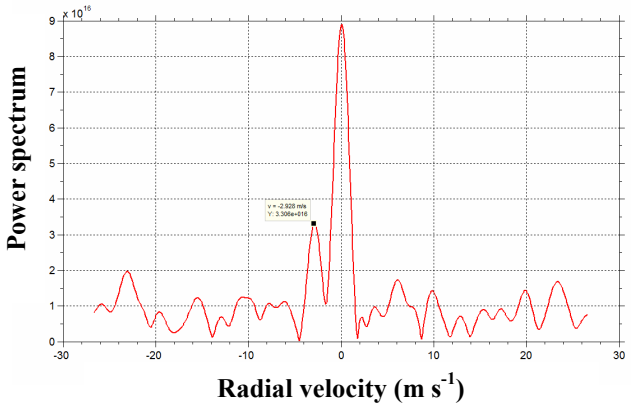


**Fig.11.** Estimation of Doppler spectrum of the spectrum weather radar signal returns mixed with a ground clutter echoes obtained form the uniform sampled part of the autocorrelation function.

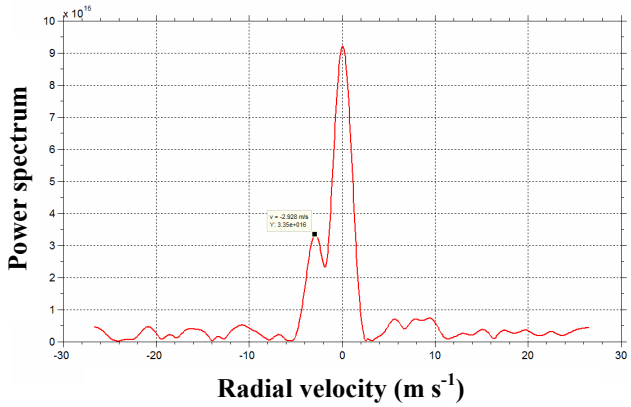


**Fig.12.** Same as figure 11, but a hamming window is applied on the correlation function before FFT, to reduce the sinc side-lobes.

To demonstrate the potentiality of the multiple-PRT for spectrum reconstruction and ground clutter filtering, a sequence of Doppler spectra is illustrated in fig.13. This sequence represents 4 spectra, at the same 12km range, separated by 1° in azimuth, and for a 4° azimuthal sector around 68.5°. This sector corresponds to a transition between ground echo and rain.

The fig.13a shows a Doppler spectrum of the rain with a strong component of ground clutter. As the antenna rotate, we observe a decrease of the ground clutter zero Doppler line between the azimuths of 67° and 69° (fig.13a to fig.13c) until wholly disappears in the azimuth 70° (fig.13d), while the rain component still remains approximately at the same spectral position (same radial velocity) and intensity.

## 5. Conclusion

The proposed multiple-PRT technique is a novel approach to mitigate the range and velocity ambiguities in a weather Doppler radar. To perform this technique it is essential to have an idea about the desired extended Nyquist interval, the unambiguous range and the number of samples needed in the considered dwell time.

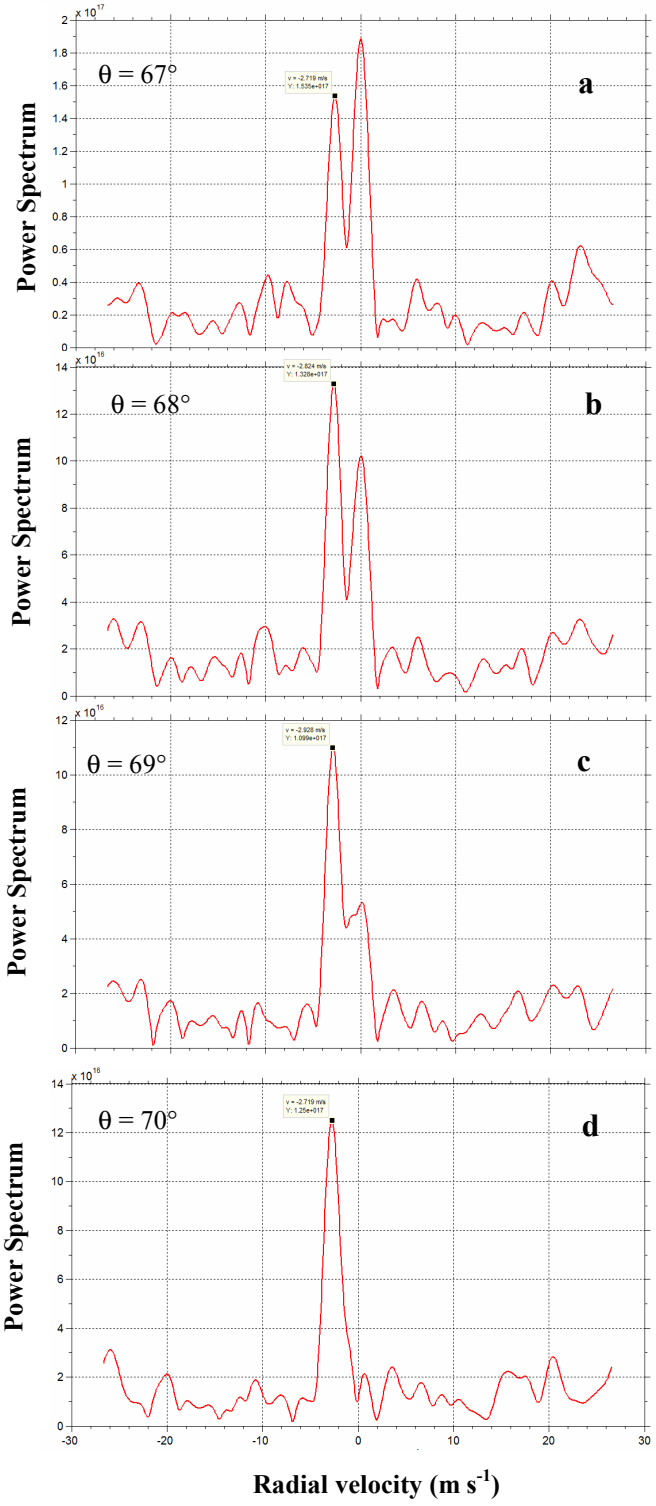


**Fig.13.** An example of sequence of estimated Doppler spectrum over 4° in azimuth. Azimuth $\theta \in [67,70]°$.

The performances of the multiple-PRT scheme have been demonstrated by a simulation approach where a 7-PRT scheme is compared to an optimum triple-PRT defined by the previous Meteo-France studies.

This simulation reveals the advantage to use the 7-PRT scheme to estimate the weather Doppler spectrum, particularly in the presence of ground clutter echoes over an extended Nyquist interval of ± 26 m $s^{-1}$. In fact, increasing the number of time periods in the multiple-

PRT scheme increases the uniform interval where the autocorrelation function is available.
Limiting the spectrum analysis to this uniform interval of the autocorrelation function allows a best Doppler power spectrum recovery. This makes possible the separation between the weather and ground clutter spectrum contributions, more accurately than the classical dealiasing algorithm. This technique enhances the precision of estimation of the mean radial velocity and gives potential investigation to develop Doppler ground clutter filters. These performances are demonstrated also by experimental results at least for weak and moderate rain (just because, during our experiment in June and July 2009 the observed phenomena were not very intense around the Abbeville radar).
Further experiment is ongoing to complement the current study with storms, to develop ground clutter filtering and to found multiple–PRT schemes with as less as possible holes in the autocorrelation function.

Acknowledgments

The authors thank Laurent Perier and Denis Feriol for their grateful help in the preparation of the experiment.

---

REFERENCES

Bousquet, O., P. Tabary, J.Parent du Châtelet, 2008: Operational Multiple-Doppler wind Retrieval Inferred from Long-Range radial Velocity Measurements. Journal Atmospheric and Oceanic Technology, **45**, 2929-2945.

Doviak, R. J., and Zrnić, 1993: Doppler radar and Weather Observations. Academic press, 562 pp.

Moiseev, D. N., C. M. Nguyen, V. Chandrasekar, 2009: Clutter Suppression for Staggered PRT Waveforms. Journal Atmospheric and Oceanic Technology, **25**, 2209–2218.

Ruzanski, E., J.C. Hubbert and V. Chandrasekar, 2008: Evaluation of simultaneous Multiple pulse Repetition Frequency Algorithm for weather radar. Journal Atmospheric and Oceanic Technology, **25**, 1166-1181.

Sachidananda, M., D.S. Zrnić, 2000: Clutter filtering and spectral Moment Estimation for Doppler weather radars Using Staggered Pulse Repetition Time (PRT). Journal Atmospheric and Oceanic Technology, **17**, 323-331.

Sachidananda, M., D.S. Zrnić, 2002: An Improved Clutter Filtering and spectral Moment Estimation Algorithm for Staggered PRT sequences. Journal Atmospheric and Oceanic Technology, **19**, 2009-2019.

Sachidananda, M., D.S. Zrnić: 2006, Ground Clutter Filtering Dual polarized, Staggered PRT sequences. Journal Atmospheric and Oceanic Technology, **23**, 1114-1130.

Tabary, P., J. Gagneux and J. Parent-Du-Châtelet, 2005: Test of a Staggered PRT Scheme for the French Radar Network. Journal Atmospheric and Oceanic Technology,**22**, 352-364.

Tabary, P., F. Guibert, L. Perier and J. Parent-Du-Châtelet, 2006: An Operational Triple-PRT Doppler Scheme for the French Radar Netwok. Journal of Atmospheric and Oceanic Technology, 1645-1656.

Torres, Sebastian, Yannick F. Dubel and D.S. Zrnić, 2004: Design, Implementation of a staggered PRT Algorithm for the WSR-88D. Journal Atmospheric and Oceanic Technology, **21**, 1389-1399.

Zrnić D. S., 1975: Simulation of Weatherlike Doppler Spectra and Signals. Journal of Applied Technology, **14**, 619-620.

Zrnić D. S., P. Mahapatra, 1985: Two Methods of Ambiguity Resolution in Pulse Doppler Weather Radars. IEEE Transactions on Aerospace and Electronic Systems, **21**, 470-483.